

Maximum-likelihood CFAR for Weibull background

R. Ravid
N. Levanon

Indexing terms: Radar, Algorithms

Abstract: A low-loss CFAR algorithm for Weibull background is discussed. The two parameters (shape and scale) of the background statistics are estimated using a maximum-likelihood algorithm. A CFAR threshold based on parameters estimated in this way exhibits a smaller variance, and hence a smaller CFAR loss, than thresholds based on other estimation algorithms such as moments or order statistics. The analysis covers both complete and censored background sample sets.

1 Introduction

The Weibull probability density function (PDF) is known to represent sea and ground clutter at low grazing angles or at high-resolution situations [1, 2]. The Weibull PDF is a two-parameter distribution, of which the Rayleigh distribution is a special case. In cases of large clutter-to-noise ratio, the clutter PDF dominates the background. This paper deals with such a situation, and assumes that the background can be described by a Weibull PDF

$$f(x) = \frac{C}{B} \left(\frac{x}{B}\right)^{C-1} \exp\left[-\left(\frac{x}{B}\right)^C\right] \quad (1)$$

where the random variable x is the output of the envelope detector, B is the scale parameter, and C is the shape parameter.

Constant false-alarm rate (CFAR) detectors for Weibull background have been suggested in the past [3–5]. The adaptive threshold was effectively based on the estimation of the scale parameter and the shape parameter, using either moments [3] or order statistics [4, 5]. Both techniques exhibit extensive CFAR loss [5]. It has also been demonstrated that the loss is related to the variance of the estimated parameters [5]. To reduce the variance, and therefore the CFAR loss, a CFAR algorithm in which the parameters are estimated using maximum likelihood, was developed and is described here. The maximum-likelihood (ML) algorithm is more computational-intensive than the other two approaches; however, modern processors may be able to handle the additional processing. Even if not implemented, the expected performances of the ML algorithm can serve as a comparative reference for the simpler algorithms.

In the following sections we will develop the ML-CFAR algorithm and analyse its performance, beginning with the simple case in which the shape parameter is known, and proceeding to the case in which both

parameters are unknown. For that general case we will show that the maximum-likelihood (ML) CFAR threshold is implemented as shown in Fig. 1, by setting the

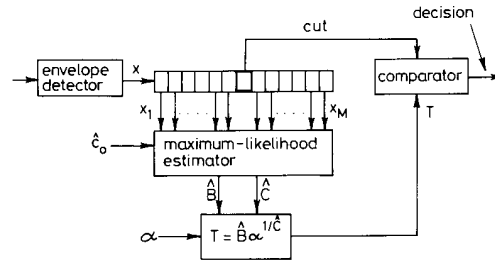


Fig. 1 Maximum-likelihood CFAR for Weibull background

adaptive threshold according to

$$T = \hat{B} \alpha^{1/\hat{C}} \quad (2)$$

The ML estimates of B and C are obtained [6] from the M background samples

$$\hat{x} = (x_1, x_2, \dots, x_M)^T \quad (3)$$

by solving iteratively for \hat{C} the equation

$$\frac{\sum_{j=1}^M x_j^{\hat{C}} \ln x_j}{\sum_{j=1}^M x_j^{\hat{C}}} - \frac{1}{\hat{C}} = \frac{1}{M} \sum_{j=1}^M \ln x_j \quad (4)$$

and using this \hat{C} , obtain \hat{B} from

$$\hat{B} = \left(\frac{1}{M} \sum_{j=1}^M x_j^{\hat{C}} \right)^{1/\hat{C}} \quad (5)$$

The coefficient α is a function of the number of reference samples M and the desired probability of false alarm P_{FA} . α is independent of the parameters B and C .

The performances of the ML CFAR will be analysed and compared against the performances of the Weber-Haykin algorithm [4], which is based on order statistics [5]. The threshold-determining algorithm and its performances will also be given for the case in which it is desired to censor a given number of the highest-ranked background samples, to gain immunity against interfering targets.

2 ML CFAR for Weibull background with known shape parameter

Our analysis will begin with the more simple case in which the shape parameter is known, and we will show

Paper 8630F (E15), first received 2nd January and in revised form 17th September 1991

The authors are with the Department of Electrical Engineering-Systems, Tel-Aviv University, Ramat Aviv, 69978 Tel-Aviv, Israel

that α can be explicitly expressed in terms of M , P_{FA} and the known C .

2.1 Uncensored ML CFAR (known C)

The background is represented by a set of M -independent identically distributed (IID) samples x_1, x_2, \dots, x_M , with a Weibull probability density function (PDF), with a known shape parameter C , and an unknown scale parameter B .

For the special case $C = 2$, the PDF becomes Rayleigh, for which it has been shown [7] that the maximum-likelihood estimator of B is

$$\hat{B} = \left(\frac{1}{M} \sum_{j=1}^M x_j^2 \right)^{1/2} \quad (6)$$

and a threshold of the form

$$T(\hat{x}) = \alpha \hat{B} \quad (7)$$

yields an optimal detector, which maximises the probability of detection for a given probability of false alarm. Such a detector is called a uniformly most powerful (UMP) test. It has also been shown [8] that the resulting probability of false alarm is given by

$$P_{FA} = \left(1 + \frac{\alpha^2}{M} \right)^{-M} \quad (8)$$

In an analogy to this special case ($C = 2$), we will use the same kind of threshold, with the ML estimate of B , when C is known but is not necessarily equal to 2. References 9 and 10 show that for such a case the ML estimator is given by

$$\hat{B} = \left(\frac{1}{M} \sum_{j=1}^M x_j^C \right)^{1/C} \quad (9)$$

yielding a threshold

$$T(\hat{x}) = \alpha \hat{B} = \alpha \left(\frac{1}{M} \sum_{j=1}^M x_j^C \right)^{1/C} \quad (10)$$

A false alarm happens when the value in the cell under test (CUT) exceeds the threshold, yielding

$$P_{FA} = \int_0^\infty P[\text{CUT} > T(\hat{x})] f_x(\hat{x}) d\hat{x} \quad (11)$$

The first term in the integrand is

$$\begin{aligned} P(\text{CUT} > T) &= \int_T^\infty f(x) dx \\ &= \int_T^\infty \frac{Cx^{C-1}}{B^C} \exp \left[-\left(\frac{x}{B} \right)^C \right] dx \\ &= \exp \left[-\left(\frac{T}{B} \right)^C \right] \end{aligned} \quad (12)$$

Substituting the threshold from eqn. 10 in eqn. 12 we obtain, for the first term in the integrand

$$P(\text{CUT} > T) = \exp \left[-\frac{\alpha^C}{M} \sum_{j=1}^M \left(\frac{x_j}{B} \right)^C \right] \quad (13)$$

The second term in the integrand of eqn. 11 is the joint PDF of the M samples, which is

$$f_x(\hat{x}) = \prod_{j=1}^M \frac{C}{B} \left(\frac{x_j}{B} \right)^{C-1} \exp \left[-\left(\frac{x_j}{B} \right)^C \right] \quad (14)$$

Inserting eqns. 13 and 14 into eqn. 11 we obtain

$$\begin{aligned} P_{FA} &= \prod_{j=1}^M \int_0^\infty \frac{C}{B} \left(\frac{x_j}{B} \right)^{C-1} \\ &\quad \times \exp \left[-\left(1 + \frac{\alpha^C}{M} \right) \left(\frac{x_j}{B} \right)^C \right] dx_j \end{aligned} \quad (15)$$

Substituting $y_j = (x_j/B)^C$ we obtain

$$P_{FA} = \prod_{j=1}^M \int_0^\infty \exp \left[-\left(1 + \frac{\alpha^C}{M} \right) y_j \right] dy_j \quad (16)$$

from which we obtain

$$P_{FA} = \left(1 + \frac{\alpha^C}{M} \right)^{-M} \quad (17)$$

Eqn. 17 indicates that the algorithm is indeed CFAR, as the false-alarm probability is independent of B . Using eqn. 17 in eqn. 10 results in a rather simple expression for the threshold

$$T(\hat{x}) = \left[(P_{FA}^{-1/M} - 1) \sum_{j=1}^M x_j^C \right]^{1/C} \quad (18)$$

2.2 Censored ML CFAR (known C)

The presence of interfering targets among the reference cells can drastically degrade the performances of the CFAR detector. To reduce this degradation, Rickard and Dillard [11] proposed to censor the $M - K$ largest cells. For the case of Rayleigh distributed samples, the maximum-likelihood estimator of B , using the K smallest cells, was shown by Epstein and Sobel [12] to be

$$\hat{B} = \left\{ \frac{1}{K} \left[(M - K)x_{(K)}^2 + \sum_{j=1}^K x_{(j)}^2 \right] \right\}^{1/2} \quad (19)$$

where

$$x_{(1)} \leq x_{(2)} \leq \dots \leq x_{(K)} \leq \dots \leq x_{(M)} \quad (20)$$

It has been shown that this estimator has the same distribution as the ML estimator of B based on K uncensored reference cells [12]. The censored ML estimator for the Rayleigh background and square-law detector was discussed by Ritcey [13].

For the Weibull background we propose to use the ML estimator of B based on the K smallest samples out of M reference samples, which was shown [9, 10] to be

$$\hat{B} = \left\{ \frac{1}{K} \left[(M - K)x_{(K)}^C + \sum_{j=1}^K x_{(j)}^C \right] \right\}^{1/C} \quad (21)$$

In References 9 and 10 it was also shown that the estimator presented in eqn. 21 has the same distribution as the ML estimator of B based on K uncensored cells. If the threshold remains as in eqn. 7, the relation between P_{FA} and α , given in eqn. 17, will apply after replacing the total number of cells M , by the highest rank used K . Thus, for the censored case we obtain the following relation between P_{FA} and T :

$$T(\hat{x}) = \left\{ (P_{FA}^{-1/K} - 1) \left[(M - K)x_{(K)}^C + \sum_{j=1}^K x_{(j)}^C \right] \right\}^{1/C} \quad (22)$$

2.3 Square-law detector

The analysis has so far assumed a linear detector, but adapting to a square-law detector is straightforward.

Note that if the random variable x is Weibull distributed with the shape parameter C , the product of a square-law detector $y = x^2$ is also Weibull, with the shape parameter $C/2$. Hence, for the uncensored case the threshold will become

$$T(\hat{y}) = \left[(P_{FA}^{-1/M} - 1) \sum_{j=1}^M y_j^{C/2} \right]^{2/C} \quad (23)$$

3 ML-CFAR for Weibull background with unknown shape parameter

When both the scale parameter and the shape parameter are unknown, they need to be estimated simultaneously from the reference samples. The adaptive threshold will be based on the estimates of B and C . In this Section we will derive the maximum-likelihood estimates of B and C , prove that the threshold described by eqn. 2 is indeed CFAR, and discuss the relation between the controlling coefficient α and the probability of false alarm P_{FA} . Unfortunately, we could not find an analytic expression for that relationship, and the results will be expressed in graphs, produced with the help of Monte-Carlo simulations.

3.1 The ML estimator of the shape and scale parameters

The derivation of the ML estimators for B and C was reported in References 6, 9 and 10. We will repeat this derivation briefly: to obtain the ML estimators, we derive the joint PDF of the M reference cells $f(\hat{x})$, differentiate its logarithm with respect to B and C , and equate to zero. The resulting set of equations can be solved iteratively to obtain the ML estimates of B and C .

Assuming independence between the reference cells, the joint PDF is

$$f(\hat{x}) = \left(\frac{C}{B^C} \right)^M \prod_{j=1}^M \left[x_j^{C-1} \exp \left(-\frac{x_j^C}{B^C} \right) \right] \quad (24)$$

from which we obtain

$$\ln f(\hat{x}) = M \ln C - MC \ln B + (C-1) \sum_{j=1}^M \ln x_j - \frac{1}{B^C} \sum_{j=1}^M x_j^C \quad (25)$$

$$\frac{\partial \ln f(\hat{x})}{\partial B} = -\frac{MC}{B} + \frac{C}{B} \sum_{j=1}^M \left(\frac{x_j}{B} \right)^C \quad (26)$$

$$\frac{\partial \ln f(\hat{x})}{\partial C} = \frac{M}{C} - M \ln B + \sum_{j=1}^M \ln x_j - \sum_{j=1}^M \left(\frac{x_j}{B} \right)^C \ln \left(\frac{x_j}{B} \right) \quad (27)$$

Equating eqn. 26 to zero yields

$$\hat{B}^C = \frac{1}{M} \sum_{j=1}^M x_j^C \quad (28)$$

Equating eqn. 27 to zero and using eqn. 28 yields

$$\frac{\sum_{j=1}^M x_j^C \ln x_j}{\sum_{j=1}^M x_j^C} - \frac{1}{M} \sum_{j=1}^M \ln x_j = \frac{1}{\hat{C}} \quad (29)$$

Eqn. 29 can be solved iteratively to yield \hat{C} , which will then be used in eqn. 28 to yield \hat{B} .

We now have to justify the choice of the threshold as described by eqn. 2. We first note from eqn. 12 that when B and C are known exactly, the probability of false alarm is

$$P_{FA} = \exp \left[-\left(\frac{T}{B} \right)^C \right] \quad (30)$$

Hence

$$T = B(-\ln P_{FA})^{1/C} \quad (31)$$

When B and C are not known exactly, and are replaced by their estimated values, which are not error-free, a given threshold yields a larger P_{FA} than predicted by eqn. 30. To compensate for that, we replace $-\ln P_{FA}$ by a parameter α , which can be verified to determine the desired P_{FA} . The threshold is therefore set according to

$$T = \hat{B} \alpha^{1/C} \quad (32)$$

For a large number of reference cells M , and relatively high P_{FA} , we indeed expect α to be only slightly higher than $-\ln P_{FA}$.

In Appendix A we will prove that the heuristic approach that led to eqn. 32 was justified, and that eqn. 32 yields a CFAR detector. Furthermore, it can also be shown that this is the only possible threshold based on the ML estimators of B and C that maintains CFAR.

Using the simulation technique discussed in Appendix B, we have obtained results for the relationship between α and P_{FA} for two values of M (16 cells and 32 cells). The results are plotted in Fig. 2. We have also added the

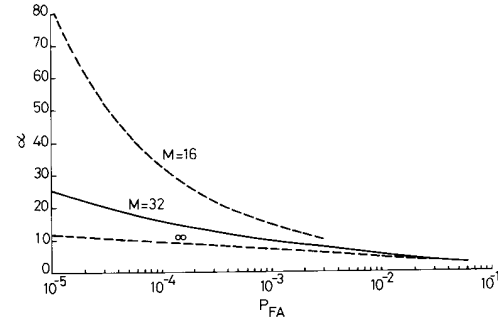


Fig. 2 α as a function of P_{FA} . The lowest curve is $-\ln(P_{FA})$

curve of $-\ln P_{FA}$, to which α converges when M tends to infinity. In Fig. 2, each point on the curve corresponding to $M = 32$ was obtained from 100 000 trials, and each point on the $M = 16$ curve was obtained from 50 000 trials. The curves are obtained using linear interpolation between the points, without smoothing.

3.2 Censored ML-CFAR (unknown C)

To provide the ML-CFAR detector with immunity against interfering targets, we resort again to the practice of censoring the highest $M - K$ samples. The improved immunity will be achieved at the expense of decreased estimation accuracy, and therefore increased CFAR loss. The ML estimators for B and C in the censored case were studied in References 6, 9 and 10, and are given by

$$\frac{(M-K)x_{(K)}^C \ln x_{(K)} + \sum_{j=1}^K x_{(j)}^C \ln x_{(j)}}{(M-K)x_{(K)}^C + \sum_{j=1}^K x_{(j)}^C} - \frac{1}{K} \sum_{j=1}^K \ln x_{(j)} = \frac{1}{\hat{C}} \quad (33)$$

$$\hat{B} = \left\{ \frac{1}{K} \left[(M-K)x_{(K)}^c + \sum_{j=1}^K x_{(j)}^c \right] \right\}^{1/c} \quad (34)$$

Contrary to the case of a known shape parameter, where the relationship between α and P_{FA} depended only on K , here we find that \hat{C} , and hence the relationship, is a function of both K and M . An example of the relationship between α and P_{FA} for $M = 32$ and various K s, is given in Fig. 3. This was obtained using the combination of

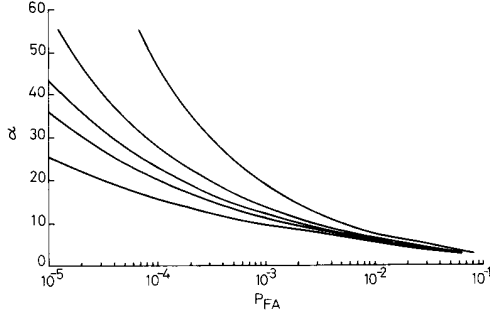


Fig. 3 α against P_{FA} for censored background sample sets. The lowest curve corresponds to $K = 32$
 $M = 32$
 $K = 20, 24, 26, 28, 32$

Monte-Carlo simulations and analytic calculations described in Appendix B. Each point is the result of 100 000 trials. The lowest curve corresponds to $K = 32$, and the uppermost curve corresponds to $K = 20$. This indicates that for a given M and P_{FA} , decreasing K requires an increase in α .

4 Probability of detection and CFAR loss

The probability of detection will be studied for the case of a fluctuating target with Rayleigh PDF. As long as we are dealing with a single-pulse case, both Swerling I and Swerling II targets are covered. With this type of target we encounter a difficulty in the cell under test (CUT). The PDF of the target plus the background (which add as vectors) cannot be obtained in a closed form. An attempt to compute P_D directly, using the exact PDF of the CUT, results in a complicated triple integral which is hard to evaluate numerically. We therefore seek an approximation which is easier to compute. We note that when the signal-to-clutter ratio is high, the contribution of the clutter to the signal in the CUT is small, and the exact PDF of that contribution is not very important. We will therefore assume that the CUT contains the Rayleigh target plus Rayleigh clutter with the same mean energy as the Weibull clutter in the reference cells. This approximation will become exact when the reference cells also exhibit a Rayleigh PDF.

4.1 Known shape parameter

When the shape parameter C is known, the threshold is based on the estimate of the scale parameter, as in eqn. 7. The probability of detection will therefore be

$$P_D = \int_0^\infty P(\text{CUT} > \alpha B) f_B(B) dB \quad (35)$$

where $f_B(B)$ is the PDF of the ML estimator of B , given in eqn. 76. The probability of the CUT crossing a threshold

T is obviously

$$P(\text{CUT} > T) = \int_T^\infty f_{\text{CUT}}(y) dy \quad (36)$$

As indicated above, we will assume a fluctuating target with Rayleigh PDF, and mean power of B_t^2 . The clutter in the CUT will be approximated by a Rayleigh PDF with the same mean power as the Weibull clutter in the reference cells. The mean clutter power B_c^2 will be related to the scale parameter B , as

$$B_c^2 = B^2 \Gamma \left(1 + \frac{2}{C} \right) \quad (37)$$

Since both target and clutter in the CUT are Rayleigh distributed, the PDF of the CUT will also be Rayleigh distributed

$$f_{\text{CUT}}(y) = \frac{y}{B^2 \Gamma \left(1 + \frac{2}{C} \right) + B_t^2} \exp \left[\frac{-y^2}{B^2 \Gamma \left(1 + \frac{2}{C} \right) + B_t^2} \right] \quad (38)$$

Defining a signal-to-clutter ratio (SCR)

$$\text{SCR} = \frac{B_t^2}{B^2 \Gamma \left(1 + \frac{2}{C} \right)} \quad (39)$$

and using it and eqn. 38 in eqn. 36, we will obtain

$$P(\text{CUT} > \alpha \hat{B}) = \exp \left[\frac{-(\alpha \hat{B})^2}{B^2 (1 + \text{SCR}) \Gamma \left(1 + \frac{2}{C} \right)} \right] \quad (40)$$

Using eqns. 76 and 40 in eqn. 35 we can find P_D

$$P_D = \int_0^\infty \exp \left[\frac{-(\alpha y)^2}{B^2 (1 + \text{SCR}) \Gamma \left(1 + \frac{2}{C} \right)} \right] \left(\frac{M}{B^C} \right)^M \times \frac{C y^{CM-1}}{(M-1)!} \exp \left(\frac{-M y^C}{B^C} \right) dy \quad (41)$$

Substituting

$$z = \frac{M y^C}{B^C} \quad (42)$$

we obtain the result for the probability of detection when $\text{SCR} \gg 1$:

$$P_D = \frac{1}{(M-1)!} \int_0^\infty z^{M-1} \times \exp \left[\frac{-\alpha^2}{(1 + \text{SCR}) \Gamma \left(1 + \frac{2}{C} \right)} \left(\frac{z}{M} \right)^{2/C} - z \right] dz \quad (43)$$

For the special case of Rayleigh clutter (in which $C = 2$) this integral can be solved explicitly, reducing to the well known result

$$P_D = \left[1 + \frac{\alpha^2}{M(1 + \text{SCR})} \right]^{-M} \quad (44)$$

Eqn. 43 is an approximate expression, because despite the fact that the clutter in the reference cells is Weibull distributed, in the CUT we have assumed it to be Rayleigh distributed (with the same mean power). In order to

check the accuracy of this approximation, we compare the P_D calculated using eqn. 43 with the Monte-Carlo simulation in which the CUT contained Weibull clutter (and a Rayleigh target). The results are given in Fig. 4, in

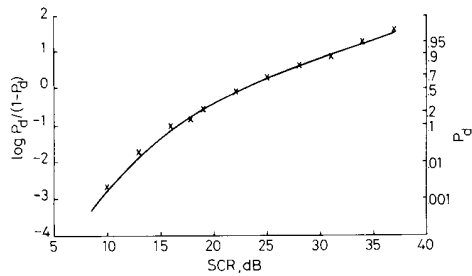


Fig. 4 Probability of detection as a function of the signal-to-clutter ratio. The solid curve is the theoretical approximation in which the cell under test (CUT) is assumed to contain a target plus Rayleigh background. The dots represent results of Monte-Carlo experiments, in which the CUT contained the target plus the correct Weibull background
 $P_{FA} = 1 \times 10^{-5}$
 $C = 1$
 $M = 16$

which the curve represents eqn. 43. The individual points are each obtained from 1000 Monte-Carlo trials. For a low SCR we expect the actual P_D to be somewhat higher than predicted by eqn. 43. The longer tail of the Weibull PDF of the clutter in the CUT will cause more threshold crossings. This is seen in Fig. 4, where the points are systematically slightly above the curve for low SCR. We thus conclude that the expression in eqn. 43 accurately describes the probability of detection of ML CFAR, when the background is Weibull distributed with any (known) shape parameter C , the target is Rayleigh fluctuating, and $SCR \gg 1$. It is also accurate for any SCR when $C \rightarrow 2$.

Note that eqn. 43 applies also to the censored case, in which the scale parameter is estimated by eqn. 21. The only change in eqn. 43 will be to replace the number of reference cells M by the highest rank used $-K$.

Fig. 5 contains numerical solutions of eqn. 43 for $P_{FA} = 10^{-5}$ and $M = 16$ reference cells, for several values

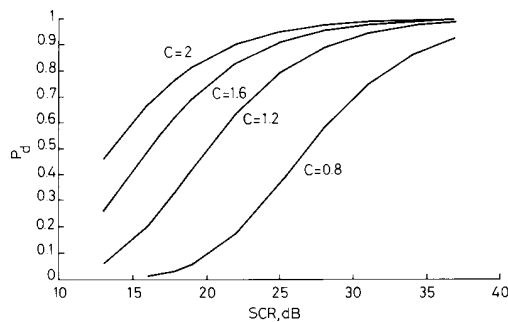


Fig. 5 Performance of the ML-CFAR for various (known) shape parameters
 $P_{FA} = 1 \times 10^{-5}$, 16 cells

of the shape parameter C . As C gets smaller, the clutter PDF has a longer tail, which forces an increase in the adaptive threshold. This explains part of the correspond-

ing drop in P_D . This effect of C on P_D should be observed also in a fixed-threshold (non-CFAR) detector. The other cause for the drop in P_D as C decreases, is the reduced accuracy in estimating B . This effect is found only in the CFAR detector. In order to separate the two effects, we will next calculate the dependence on C of the CFAR loss, rather than the probability of detection.

4.2 CFAR loss (known C)

The CFAR loss is the ratio between the SCR required to achieve a specified P_D and P_{FA} , and the SCR of the non-CFAR case, in which the clutter level is known and the threshold is a constant, designated as T_∞ . In the non-CFAR case (Rayleigh target, Weibull clutter), the following two relationships hold:

$$P_{FA} = \exp\left(\frac{-t_\infty^C}{B^C}\right) \quad (45)$$

$$P_D = \exp\left[\frac{-\left(\frac{t_\infty}{B}\right)^2}{\left(1 + SCR\right)\Gamma\left(1 + \frac{2}{C}\right)}\right] \quad (46)$$

from which we obtain the non-CFAR triple relationship between SCR, P_{FA} and P_D

$$SCR_\infty = \frac{(\ln(1/P_{FA}))^{2/C}}{(\ln(1/P_D))\Gamma\left(1 + \frac{2}{C}\right)} - 1 \quad (47)$$

When the CFAR detector is employed, we find the SCR for a given P_{FA} , P_D and K by first calculating α from the required P_{FA} using eqn. 17; using that α , eqn. 43 is solved iteratively (using K in place of M) for the SCR. The CFAR loss is defined by the quotient

$$CFAR \text{ loss} = \frac{SCR(P_{FA}, P_D, C, K)}{SCR_\infty(P_{FA}, P_D, C)} \quad (48)$$

Using this procedure we have calculated the CFAR loss as a function of C , for the case of $K = 16$, $P_D = 0.5$ and $P_{FA} = 10^{-5}$. The results are presented in Fig. 6. By comparing Figs. 5 and 6 we note, for example, that the

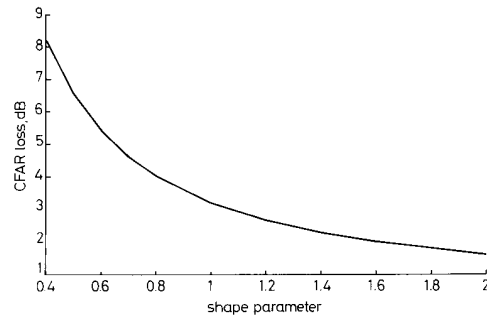


Fig. 6 The CFAR loss of the ML-CFAR against the (known) shape parameter
 Known C , $P_{FA} = 1 \times 10^{-5}$
 $P_D = 0.5$
 $K = 16$

increase of 13 dB necessary to maintain $P_D = 0.5$ as C drops from 2 to 0.8 (Fig. 5), is constructed from about 2.4 dB additional CFAR loss (Fig. 6), and a balance of

10.6 dB increase, that would have been required by a fixed-threshold detector.

Another interesting observation from Fig. 6 is the approximation

$$\text{CFAR loss}(C_1)_{(\text{dB})} \approx \frac{C_2}{C_1} \text{CFAR loss}(C_2) \quad (49)$$

which can also be justified analytically.

Fig. 7 shows the dependence of the CFAR loss on the number of reference cells used. The abscissa is M in the

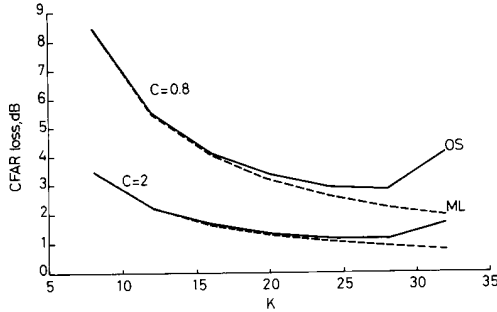


Fig. 7 CFAR loss as a function of reference cells used out of a total of 32 cells
 $P_{FA} = 1 \times 10^{-5}$

uncensored case, or K (out of $M = 32$) in the censored case. The CFAR loss for the ML CFAR is compared to that of Rohling's order statistics (OS) CFAR [14]. A similar comparison for a Rayleigh clutter ($C = 2$) was reported in Reference 15. In Fig. 7 we have added the results for $C = 0.8$. In the censored case the losses of the ML CFAR are a function only of K , while the losses of the OS CFAR are a function of both K and M . Fig. 7 demonstrates that for $K < 3M/4$, the CFAR losses of both algorithms are comparable.

4.3 Unknown shape parameter

When both B and C are estimated by the maximum-likelihood algorithm, their distribution is not available in a closed form, to allow calculation of the P_D in a similar way to the procedure described by eqn. 35 for the 'known C ' case. Instead of using an expression such as eqn. 35 we will use an approximation based on $E(T)$, the expected value of the threshold:

$$P_D = \int_0^{\infty} P(\text{CUT} > T) f_T(\hat{x}) d\hat{x} \approx P[\text{CUT} > E(T)] \quad (50)$$

The rationale behind this approximation can be explained with the help of Fig. 8, which presents the simulation results of a typical case. The dotted Gaussian-like curve is the PDF of the threshold. The solid line is the probability distribution $P(\text{CUT} > T)$, when the CUT contains only clutter, and the dashed line is $P(\text{CUT} > T)$ when the CUT contains target plus clutter. The parameters used to generate Fig. 8 were $C = 2$, $M = 64$, $\text{SCR} = 25$ dB. Fig. 8 demonstrates that $P(\text{CUT} > T)$ for the 'target plus clutter' case is relatively constant over the narrow interval of T in which its PDF is of any significance. Therefore $P(\text{CUT} > T)$ can be replaced by its value at $E(T)$. The same is not true for the 'clutter only' case. The curve $P(\text{CUT} > T)$ in the 'clutter only' case drops rapidly during the relevant interval of values of the threshold T .

With the assumption expressed in eqn. 50, the procedure of calculating P_D is to determine, by simulations, the expected threshold $E(T)$ for a given situation (M , B , C , P_{FA}). With $E(T)$ available, the probability of detection

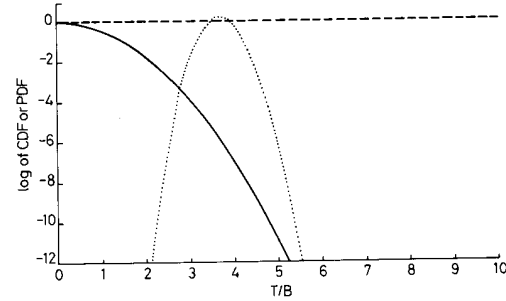


Fig. 8 1 - CDF of the cell under test with (---) and without (—) a target, and the PDF of the normalised threshold (.....)

(assuming again Rayleigh target and Rayleigh clutter in the CUT) is given by

$$P_D = \exp \left[\frac{-\left(\frac{E(t)}{B}\right)^2}{(1 + \text{SCR})\Gamma\left(1 + \frac{2}{C}\right)} \right] \quad (51)$$

from which we extract the required SCR

$$\text{SCR} = \frac{E^2(T)}{B^2 \ln\left(\frac{1}{P_D}\right)\Gamma\left(1 + \frac{2}{C}\right)} - 1 \quad (52)$$

In the non-CFAR case we will obtain the same expression, except for replacing $E(T)$ by the constant threshold T_∞ . Thus

$$\text{SCR}_\infty = \frac{T_\infty^2}{B^2 \ln\left(\frac{1}{P_D}\right)\Gamma\left(1 + \frac{2}{C}\right)} - 1 \quad (53)$$

The CFAR loss is, therefore, approximately

$$\text{CFAR loss} = \frac{\text{SCR}}{\text{SCR}_\infty} \approx \frac{E^2(T)}{T_\infty^2} \quad (54)$$

Note that this approach for approximating the CFAR loss was also used by Rohling [14]. We have checked the approximation for an unfavourable case: $M = 16$, $P_{FA} = 10^{-5}$, $P_D = 0.5$ and $C = 1$. The required SCR (from simulation) was 37.8 dB. The required SCR for the non-CFAR case is 19.8 dB, hence the exact CFAR loss is 18 dB. The CFAR loss obtained from the approximation in eqn. 54 was 18.8 dB. Thus for this unfavourable case the error was 0.8 out of 18 dB. Note that the number of Monte-Carlo trials required for the approximation is smaller, because they do not extend beyond finding the average threshold.

4.4 Performance comparison between the ML CFAR and the WH CFAR

The performances of the ML CFAR in the case of unknown C will be compared to the performances of the Weber-Haykin (WH) algorithm [4, 5]. According to the WH algorithm, the threshold is set using the i th and j th

ranked reference cells:

$$T = x_{(i)}^{1-\beta} x_{(j)}^{\beta} \quad (55)$$

As pointed out by Levanon and Shor [5], this threshold is also of the form

$$T = \hat{B}\alpha^{1/C} \quad (56)$$

where $\hat{B} = x_{(i)}$ and \hat{C} is the percentile estimator suggested by Dubey [16]. Dubey found that the optimal values for i and j are the closest integers to $0.1673M$ and $0.9737M$, respectively. We have used these values in the comparison.

In order to run the comparison we used α from Fig. 2, but we also needed β for the WH algorithm. β as a function of P_{FA} for $M = 16$ ($i = 3, j = 16$) and $M = 32$ ($i = 5, j = 31$) reference cells is given in Fig. 9. The CFAR losses

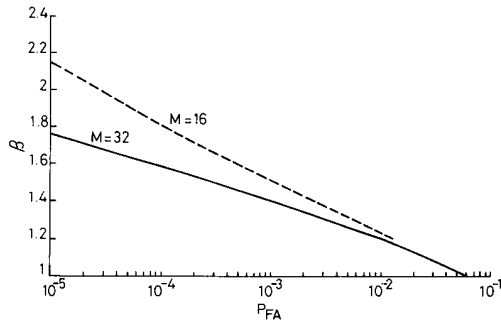


Fig. 9 The coefficient β of the Weber-Haykin CFAR algorithm.

--- $M = 16, i = 3, j = 16$
 — $M = 32, i = 5, j = 31$

were calculated using the approximation in eqn. 54, which applies also to the WH algorithm. The results for $M = 16$ and 32 and for $C = 1$ and 2 , are presented in Figs. 10 and 11. In these two figures, the solid curve cor-

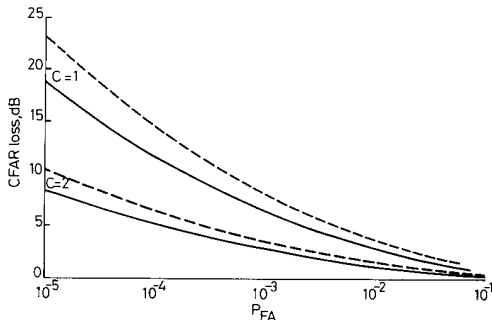


Fig. 10 CFAR loss of the maximum-likelihood algorithm (—) and the Weber-Haykin algorithm (---), for $M = 16$ cells, and $C = 1$ and 2

responding to the ML CFAR is the lower curve, indicating that its CFAR loss is always smaller than the CFAR loss of the WH CFAR (dashed curve).

4.5 Comparison between ML CFAR and WH CFAR (censored case)

When the highest ranked cells are censored to protect the algorithms from interfering targets, the estimates of the parameters are poorer, causing an increased CFAR loss. The two algorithms were compared also in the censored case, in which the lowest 26 cells out of a total of 32 cells

were used. In the WH algorithm this meant $i = 5$, and $j = 26$. The corresponding α and β values as functions of the P_{FA} are presented in Figs. 3 and 12. The CFAR loss

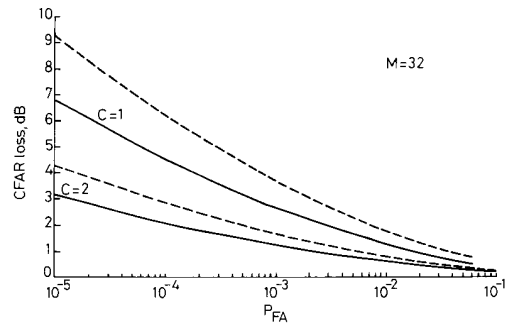


Fig. 11 CFAR loss of the maximum-likelihood algorithm (—) and the Weber-Haykin algorithm (---), for $M = 32$ cells and $C = 1$ and 2

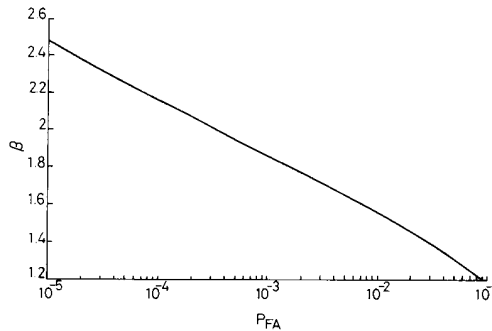


Fig. 12 The coefficient β of the Weber-Haykin CFAR algorithm

$M = 32$
 $i = 5$
 $j = 26$
 $K = 26$

curves for $C = 1$ and 2 are presented in Fig. 13. Note that the ML CFAR exhibits a smaller loss also in the censored case.

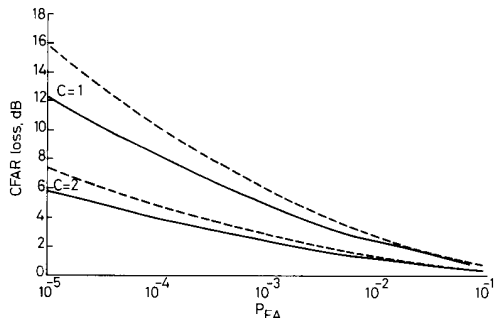


Fig. 13 CFAR loss of the maximum-likelihood algorithm (—) and the Weber-Haykin algorithm (---). In both algorithms the highest rank used is 26 (out of a total of 32 cells). The Weibull shape parameters are $C = 1$ and 2

$M = 32$
 $K = 26$

5 Conclusions

We have described a CFAR algorithm for Weibull background, based on a maximum-likelihood estimator of the shape and scale parameters of the Weibull PDF. The

algorithm, exhibits a lower CFAR loss than the Weber–Haykin (WH) algorithm, in which the two parameters are estimated using order statistics. Since the WH algorithm was known to exhibit a lower loss than the moments estimator, we can claim that the maximum-likelihood CFAR for the Weibull background described in this paper, yields the lowest CFAR loss of all the known CFAR algorithms for Weibull background. However, this does not mean that the ML algorithm maximises the probability of detection for a given probability of false alarm.

The loss improvement over the WH algorithm should be weighted against the computational complexity. The iterative solution of eqn. 33 is more difficult to implement than the sorting required by the WH algorithm. The criterion for halting the iterations was a step in C smaller than $1/20$ of the theoretical standard deviation of C . This would entail a CFAR loss increase smaller than 0.05 dB. With that halting criterion, when the initial guess of C was correct, the average number of iterations was 4.4. When the correct C was 2 and the first guess was $C = 1$, the average number of iterations was 6.9.

It can be shown that the algorithm presented in this paper exhibits a CFAR property for other background distributions, in particular the log-normal distribution. However, its performances in the presence of log-normal background are inferior to the performances of the 'log- t ' detector [17], which is a maximum-likelihood CFAR algorithm matched to log-normal background. In fact, every CFAR detector for Weibull background is also CFAR for log-normal background and vice versa.

6 References

- 1 SCHLEHER, D.C.: 'Radar detection in Weibull clutter', *IEEE Trans.*, 1976, **AES-12**, (6), pp. 736–743
- 2 SEKINE, M., et al.: 'Weibull distributed sea clutter', *IEE Proc. F., Radar & Signal Process.*, 1983, **130**, (5), p. 476
- 3 HANSEN, V.G.: 'Constant false alarm rate processing in search radar', *IEE Conf. Publ. 105* (IEE London, October 1973), pp. 325–332
- 4 WEBER, P., and HAYKIN, S.: 'Ordered statistics CFAR for two-parameter distributions with variable skewness', *IEEE Trans.*, 1985, **AES-21**, (6), pp. 819–821
- 5 LEVANON, N., and SHOR, M.: 'Order statistics CFAR for Weibull background', *IEE Proc. F., Radar & Signal Process.*, 1990, **137**, (3), pp. 157–162
- 6 COHEN, A.C., and WHITTEN, B.J.: 'Parameter estimation in reliability and life span models' (Marcel Dekker, New York, 1988)
- 7 GRIEVE, P.J.: 'The optimum constant false alarm probability detector for relatively coherent multichannel signals in Gaussian noise of unknown power', *IEEE Trans.*, 1977, **IT-23**, (6), pp. 708–721
- 8 FINN, H.M., and JOHNSON, R.S.: 'Adaptive detection mode with threshold control as a function of spatially sampled clutter-level estimates', *RCA Review*, 1968, **29**, pp. 414–464
- 9 HARTER, H.L., and MOORE, A.H.: 'Maximum-likelihood estimation of the parameters of gamma and Weibull populations from complete and from censored samples', *Technometrics*, 1965, **7**, (4), pp. 639–643
- 10 COHEN, A.C.: 'Maximum likelihood estimation in the Weibull distribution based on complete and censored samples', *Technometrics*, 1965, **7**, (4), pp. 579–588
- 11 RICKARD, J.T., and DILLARD, G.M.: 'Adaptive detection algorithms for multiple target situations', *IEEE Trans.*, 1977, **AES-13**, (4), pp. 338–343
- 12 EPSTEIN, B., and SOBEL, M.: 'Life testing', *J. Am. Statist. Assoc.*, 1953, **48**, pp. 486–502
- 13 RITCEY, J.A.: 'Performance analysis of the censored mean-level detector', *IEEE Trans.*, 1986, **AES-22**, (4), pp. 443–454
- 14 ROHLING, H.: 'Radar CFAR thresholding in clutter and multiple target situation', *IEEE Trans.*, 1983, **AES-19**, (4), pp. 443–454
- 15 SHOR, M., and LEVANON, N.: 'Performances of order statistics CFAR', *IEEE Trans.*, 1991, **AES-27**, (2), pp. 214–224

16 DUBEY, S.D.: 'Some percentile estimators for Weibull parameters', *Technometrics*, 1967, **9**, pp. 119–129

17 GOLDSTEIN, G.B.: 'False-alarm regulation in log-normal and Weibull clutter', *IEEE Trans.*, 1973, **AES-9**, (1), pp. 84–92

7 Appendices

7.1 A test for the CFAR property

The general expression for the P_{FA} in the case of Weibull background is given in eqn. 11 and 12, which, when combined, appear as

$$P_{FA} = \int_0^{\infty} \exp \left\{ - \left[\frac{T(\hat{x})}{B} \right]^C \right\} f_x(\hat{x}) d\hat{x} \quad (57)$$

where the PDF is given in eqn. 14 and rewritten here as

$$f_x(\hat{x}) = \prod_{j=1}^M \frac{C}{B} \left(\frac{x_j}{B} \right)^{C-1} \exp \left[- \left(\frac{x_j}{B} \right)^C \right] \quad (58)$$

Substituting

$$y_j = \left(\frac{x_j}{B} \right)^C \quad (59)$$

we obtain

$$f_y(\hat{y}) = \prod_{j=1}^M \exp(-y_j) \quad (60)$$

Using eqns. 59 and 60 in eqn. 57 we obtain

$$P_{FA} = \int_0^{\infty} \exp \left\{ - \left[\frac{T(B\hat{y}^{1/C})}{B} \right]^C \right\} \prod_{j=1}^M \exp(-y_j) dy_j \quad (61)$$

where

$$T(B\hat{y}^{1/C}) \text{ means } T(By_1^{1/C}, \dots, By_M^{1/C})$$

For the method to be CFAR, P_{FA} should be independent of both B and C . A necessary and sufficient condition for eqn. 61 to be independent from both B and C is to demand that

$$\left[\frac{T(B\hat{y}^{1/C})}{B} \right]^C = T(\hat{y}) \quad (62)$$

or equivalently

$$\left[\frac{T(\hat{x})}{B} \right]^C = T \left[\left(\frac{\hat{x}}{B} \right)^C \right] \quad (63)$$

Before we can apply this test to the threshold suggested in eqn. 32, we also need to prove that the maximum-likelihood estimates of B and C obey

$$\hat{B} \left[\left(\frac{\hat{x}}{\hat{\beta}} \right)^\gamma \right] = \frac{[\hat{B}(\hat{x})]^\gamma}{\hat{\beta}^\gamma} \quad (64)$$

$$\hat{C} \left[\left(\frac{\hat{x}}{\hat{\beta}} \right)^\gamma \right] = \frac{\hat{C}(\hat{x})}{\gamma} \quad (65)$$

To prove eqns. 64 and 65, we note that the likelihood eqns. 26 and 27, after being equated to zero, are both functions of the format

$$g \left[\left(\frac{x_j}{\hat{\beta}} \right)^C \right] = 0 \quad (66)$$

If the samples x_j are transformed into $(x_j/\hat{\beta})^\gamma$, the new solutions of the likelihood equations \hat{B}' and \hat{C}' , will satisfy

$$\left[\frac{\left(\frac{x_j}{\hat{\beta}} \right)^\gamma}{\hat{B}'} \right]^{C'} = \left(\frac{x_j}{\hat{\beta}} \right)^C \quad (67)$$

or

$$\gamma \hat{C} = \hat{C} \quad (68)$$

$$(\hat{B})^C \beta^{C'} = (\hat{B})^C \quad (69)$$

yielding

$$\hat{C} = \frac{\hat{C}}{\gamma} \quad (70)$$

$$\hat{B} = \frac{\hat{B}^\gamma}{\beta^\gamma} \quad (71)$$

which are equivalent to eqns. 65 and 64 respectively.

Having proven eqns. 64 and 65, we are now ready to test whether the threshold

$$T(\hat{x}) = \hat{B}(\hat{x})\alpha^{1/C(\hat{x})} \quad (72)$$

has the property required in eqn. 63. Replacing \hat{x} by $(\hat{x}/B)^C$ in eqn. 72, and using eqns. 64 and 65, we obtain

$$\begin{aligned} T\left[\left(\frac{\hat{x}}{B}\right)^C\right] &= \hat{B}\left[\left(\frac{\hat{x}}{B}\right)^C\right]\alpha^{1/C((\hat{x}/B)^C)} \\ &= \frac{[\hat{B}(\hat{x})]^C}{B^C} \alpha^{C/C(\hat{x})} \\ &= \left[\frac{\hat{B}(\hat{x})\alpha^{1/C(\hat{x})}}{B}\right]^C \\ &= \left[\frac{T(\hat{x})}{B}\right]^C \end{aligned} \quad \text{QED} \quad (73)$$

7.2 Determining $P_{FA}(\alpha, M)$ by Monte-Carlo simulations

An explicit expression for the P_{FA} is difficult to obtain because it requires a knowledge of the distribution of the ML estimators of B and C . The asymptotic distribution, known to be normal, can be used, but the result will be accurate only for a large number of reference cells. We therefore relied on simulations to obtain $P_{FA}(\alpha, M)$.

Straightforward Monte-Carlo simulations will require a huge number of trials if small values of P_{FA} are to be simulated. Suppose an event with probability p is simulated, and p is to be estimated by the number of events over the number of trials. The relative accuracy of such an estimator is

$$\frac{\text{STD}(\hat{p})}{p} \approx \frac{1}{\sqrt{mp}} \quad (74)$$

If the desired accuracy is 10%, the number of trials m will have to be $100/p$. To evaluate the performances for $P_{FA} = 10^{-5}$ will require 10^7 Monte-Carlo trials.

Fortunately, in our case part of the process can be described in a closed form, thus decreasing the number of

required trials by two to three orders of magnitude. The detection process consists of two ingredients: the reference cells, from which we determine the adaptive threshold, and the cell under test (CUT). We do not have a closed-form expression for the statistics of the adaptive threshold, but we do know the statistics of the CUT. We can use this fact and randomly generate only the reference cells, and from them the adaptive threshold. Given the threshold, the probability of the CUT exceeding it is given by eqn. 12. Thus, if we conduct m Monte-Carlo trials, and therefore generate m adaptive thresholds $\{T_j\}$, $j = 1, 2, \dots, m$, the estimated probability of false alarm will be given by

$$\begin{aligned} \hat{P}_{FA} &= \frac{1}{m} \sum_{j=1}^m P(\text{CUT} > T_j) \\ &= \frac{1}{m} \sum_{j=1}^m \exp\left[-\left(\frac{T_j}{B}\right)^C\right] \end{aligned} \quad (75)$$

C and B in eqn. 75 should be the ones used in generating the reference samples. The result, however, should be independent of C and B . This estimator for P_{FA} can easily be shown to be unbiased. Its variance is difficult to compute because it requires a knowledge of the threshold distribution. However, we can obtain some idea about its performance by checking the variance of this estimation technique for the simpler case of a known shape parameter. When the shape parameter is known, the PDF of the ML estimator of B was shown by Harter and Moore [9] to be

$$f_B(y) = \left(\frac{M}{B^C}\right)^M \frac{C}{(M-1)!} y^{CM-1} \exp\left(-\frac{My^C}{B^C}\right) \quad (76)$$

From the PDF of \hat{B} we can obtain the PDF of $T = \alpha\hat{B}$. From this PDF, and from eqn. 75 the variance of the estimated P_{FA} will be

$$\text{Var}(P_{FA}) \approx \frac{1}{m} \left(1 + \frac{2\alpha^C}{M}\right)^{-M} \quad (77)$$

where M is the number of cells and m is the number of trials. For $P_{FA} = 10^{-5}$, $M = 16$ and $C = 2$, it is seen that 13000 trials are needed in order to achieve 10% estimation accuracy. This is about three orders of magnitude smaller than the 10^7 trials required in a straightforward Monte-Carlo simulation. For the case of unknown shape parameter, the reduction in the number of trials is less dramatic. When $P_{FA} = 10^{-5}$, $M = 16$ and $C = 2$ (unknown to the estimator), the number of Monte-Carlo trials necessary to obtain a 10% estimation accuracy of the P_{FA} , was 6×10^4 . However, this is still a big improvement over the 10^7 trials required in the straightforward approach.